



Contents lists available at ScienceDirect

## Arabian Journal of Chemistry

journal homepage: [www.ksu.edu.sa](http://www.ksu.edu.sa)

# Ultrasonic-assisted hydrothermal fabrication of selenium nanorods and their anticancer properties in prostate cancer cells and associated signaling pathway

Du Shen<sup>a</sup>, Shaosan Kang<sup>b,\*</sup>

<sup>a</sup> College of Clinic Medicine, North China University of Science and Technology, Tangshan 063000, China

<sup>b</sup> Department of Urology, North China University of Technology Affiliated Hospital, Tangshan 063000, China

## ARTICLE INFO

## Keywords:

Synthesis  
Selenium nanorod  
Characterization  
Prostate cancer  
Signaling

## ABSTRACT

This paper describes some useful information on the ultrasonic-assisted hydrothermal fabrication of selenium nanorods (abbreviated as SeNRs) and their potential anticancer activity. The synthesis of SeNRs was confirmed and their selective anticancer activity against DU-145 cells as a standard prostate cancer cell line and human prostate normal cell line, RWPE-1 were assessed. The result of the FTIR study revealed the bending and stretching vibration of the Se-O bond. UV-vis spectroscopy data displayed a sharp maximum absorption ( $\lambda_{max}$ ) peak at 298 nm and the TEM image demonstrated that Se nanostructures had a rod-shaped morphology with lengths ranging from 50 to 100 nm and a diameter of around 10 nm. DLS data displayed that SeNRs had an average size of 204.68 nm and a zeta potential value of  $-37.29$  mV. Then,  $IC_{50}$  concentration of SeNRs against DU-145 and RWPE-1 cell lines were calculated to be about  $15 \mu\text{g/mL}$  and  $50.06 \mu\text{g/mL}$ , respectively, at 24 h. Also, it was deduced that SeNRs triggered their anticancer activity through the induction of membrane leakage, oxidative stress, apoptosis by overexpression of Bax/Bcl-2 ratio and caspase-9, -8, -3, and downexpression of AKT, PI3K, and mTOR mRNA and proteins, which was further verified by pre-incubation of cells with PI3K inhibitor, LY294002. Thus, the synthesized SeNRs can be used and developed as an effective nanostructure for the treatment of prostate cancer in future studies.

## 1. Introduction

One-dimensional (1-D) nanomaterials including nanowires, nanorods (NRs), or nanotubes have received great interest recently because of their unique physical, chemical, and medical characteristics (Kuchibhatla et al., 2007; Shin et al., 2023). The biomedical features of 1-D nanostructures, such as high drug loading potency, extended blood circulation, interaction with tumor cells, selective cellular uptake, potent photothermal capability, and chemical tunability have facilitated their capacity for biomedical implementations, specifically in cancer therapy (Shin et al., 2023). It has been reported that enhancing the cytotoxicity of cancer chemotherapeutics can be achieved through their combination with NR-mediated hyperthermia (Hauck et al., 2008; Shukla et al., 2020; Liao et al., 2015). Furthermore, Hasannia et al. (Hasannia et al., 2022) reported that doxorubicin-hybrid NRs could facilitate targeted drug delivery and imaging of metastatic tumor cells. Also, Kang et al. (Kang et al., 2022) showed that rhodium-tellurium NRs

synthesized through galvanic replacement-polyol regrowth are potential candidates for achieving dual-modal cancer thermo-dynamic therapy. Therefore, the study of synthesis and anticancer effects of inorganic NRs can be recognized as a potential research field for nanotechnologists.

A vital trace element called selenium (Se), which is incorporated into selenoproteins, regulates a variety of important cellular processes and is essential for maintaining human health (Rayman, 2012). The extensive *in vitro* and *in vivo* evidence indicated that Se nanostructures mitigate the proliferation of various types of cancers (Ahmad et al., 2015; Alkhubayri et al., 2020; Gayathri et al., 2023). For example, Gao et al. (Gao et al., 2022) demonstrated that functionalized Se nanomaterials are able to trigger anti-colon carcinoma activity mediated by apoptosis and cell cycle arrest. Additionally, Wang et al. (Wang et al., 2022) reported that green synthesized Se nanoparticles induce apoptosis as well as autophagy in gastric cancer cells mediated by regulating the PI3K/Akt/mTOR signaling pathway. Furthermore, lactoferrin-modified bio-synthesized Se nanostructures were shown to serve as a suitable

\* Corresponding author at: No 21. Bohai Avenue, Caofeidian, New Town, Tangshan 063000, China.

E-mail address: [Shaosankang12@outlook.com](mailto:Shaosankang12@outlook.com) (S. Kang).

<https://doi.org/10.1016/j.arabjc.2024.105714>

Received 31 January 2024; Accepted 5 March 2024

Available online 6 March 2024

1878-5352/© 2024 The Authors. Published by Elsevier B.V. on behalf of King Saud University. This is an open access article under the CC BY-NC-ND license (<http://creativecommons.org/licenses/by-nc-nd/4.0/>).

candidate for the induction of apoptosis in several human cancer cells (El-Fakharany et al., 2023). Although different routes for the synthesis of Se nanostructure have been reported (Bisht, Phalswal, and Khanna, 2022), the hydrothermal method seems to be a potential, simple and inexpensive approach for synthesizing SeNRs (Chen et al., 2006). This method uses a wet-chemical process to crystallize powders into nano-materials in a sealed container following high vapor pressure at different temperatures between 100 °C and 250 °C (Chen et al., 2006). However, the aggregation tendency of synthesized NRs along with the long procedure time of the hydrothermal method make difficult the application of this method for the fabrication of NRs (Ma et al., 2006; ur Rehman et al., 2023). A combination of the hydrothermal method with ultrasonication can be a potential strategy to address these drawbacks. Therefore, hydrothermal strategy with the assistance of ultrasonication can play a key role in the formation of potential NRs for therapeutic application (Ma et al., 2006).

Although the anticancer effects of Se nanostructures have been well-reported in literature, the anticancer mechanism of SeNRs synthesized through ultrasonic-assisted hydrothermal method against prostate cancer, a common disease in Chinese males, has remained still unclear.

Prostate cancer incidence is expanding rapidly in urban areas and the mortality rate is inexpertly high in rural areas of China. According to the characteristics of prostate cancer and its stages, achievements in early detection and inhibition of prostate cancer cell proliferation are the important key to ameliorating the rate of prostate cancer survival in China (Ye and Zhu, 2015).

The phosphatidylinositol-3-kinase (PI3K)/protein kinase B (Akt)/mammalian target of rapamycin (mTOR) pathway is known as a crucial intracellular signaling pathway controlling cancer cell proliferation and associated invasion (Polivka Jr and Janku, 2014). PI3K can activate Akt known as a serine/threonine kinase, which in turn facilitates cell growth and phosphorylation of mTOR by inactivating apoptosis (Polivka Jr and Janku, 2014). Thus, growth and invasion of cancer cells can be inhibited by modulating the PI3K/Akt/mTOR signaling pathway.

Therefore, in this study to prepare SeNRs with good colloidal stability and potential anticancer effects, these nanostructures were synthesized through ultrasonic-assisted hydrothermal method. After characterization, their anticancer effects against prostate cancer cells and associated signaling pathways were assessed by different cellular and molecular assays.

## 2. Material and methods

### 2.1. Materials

Hydrazine hydrate (Cat Nr: 225819, 99.99 %), selenium dioxide (SeO<sub>2</sub>, Cat Nr: 325473, 98 %), LY294002, and 3-(4,5-dimethylthiazol-2-yl)-2,5-diphenyl-2H-tetrazolium bromide (MTT, Cat Nr: CT01-5) were purchased from Sigma-Aldrich (USA).

### 2.2. Synthesis of SeNRs

Typically, 1 ml of hydrazine (N<sub>2</sub>H<sub>4</sub>, 50 %, v/v) and 0.128 g of SeO<sub>2</sub> were mixed and transferred into a 100 ml Teflon-lined stainless steel autoclave and incubated at 110 °C for 4 h followed by cooling to room temperature. The as-synthesis particles were transferred into an ultrasonic bath (BRANSON, 1510) at room temperature for 2 h. Then, the obtained product was filtered through a millipore filter (0.45 μm), washed with double distilled water as well as alcohol, dried at 100 °C overnight, and calcinated at 400 °C for 4 h.

### 2.3. Characterization of SeNRs

Synthesized SeNRs were analyzed by UV–vis spectroscopy at the wavelength of 200–600 nm using a single beam spectrophotometer (Thermo Spectronic, GENESYS™ 8, England). Fourier-transform

infrared spectroscopy (FTIR) spectrum of SeNRs was read using a Nicolet MODEL 205 (Thermo Fisher Scientific, USA) with a wavelength range from 400 to 4000 cm<sup>-1</sup>. For the transmission electron microscopy (TEM) study, 15 μl of the sample was dropped on a copper stub and after air-drying, the images of SeNRs were captured using HITACHI H-800 (Hitachi H-800, Hitachi, Japan), operating at 80 kV. Dynamic light scattering (DLS) was used to characterize the hydrodynamic radius and zeta potential of SeNRs (0.5 mg in 20 ml ultrapure water) on a Malvern Zetasizer (Malvern Zetasizer nano ZEN3600, United Kingdom).

### 2.4. Cell culture

The DU-145 cell line and the human prostate normal cell line, RWPE-1, were obtained from American Type Tissue Collection (ATCC, USA).

Cancer and normal cells were cultured in RPMI 1640 (Gibco, USA) and DMEM (Gibco, USA) media, respectively, supplemented with 10 % heat-inactivated fetal bovine serum (FBS, Gibco, USA) and 1 % antibiotics and maintained at 37 °C with 5 % CO<sub>2</sub>. To investigate the mechanisms for SeNRs-stimulated cell death, cells were pre-incubated with the LY294002 (10 μM, a PI3K inhibitor) for 2 h, then added by IC<sub>50</sub> concentration of SeNRs for a further 24 h.

### 2.5. MTT assay

Human prostate cancer and normal cells (1 × 10<sup>4</sup> cells per well) were cultured on a 96-well plate, incubated overnight, and added by different concentrations of SeNRs (0.1–20 μg/mL) for 24 h. Afterward, 10 μl of MTT dye (5 mg/mL) was added and incubated for 4 h. Then, the media were removed and replaced with 100 μl of DMSO and incubated for 15 min. Finally, the plates were read at 570 nm using a microplate reader (Bio-Tek, Winooski, USA).

### 2.6. Lactate dehydrogenase (LDH) cytotoxicity assay

The LDH assay was done based on the protocols provided with the kit (TOX7-1KT, Sigma-Aldrich). Briefly, after the incubation of the cells with IC<sub>50</sub> concentration of SeNRs determined by MTT assay, aliquots of the medium were removed and mixed with LDH reaction mixture for 30 min in the dark. After the stop of the reaction by 1 N HCl, the absorbance of the samples was read spectrophotometrically at 490 nm using a microplate reader (Bio-Tek, Winooski, USA).

### 2.7. Intracellular ROS measurement assay

The level of intracellular ROS generation was calculated by the method described previously (Sharma, Anderson, and Dhawan, 2012) using 2,7-dichlorofluorescein diacetate (DCFDA; Sigma-Aldrich) dye. Briefly, cells were seeded, exposed to SeNRs (IC<sub>50</sub> concentration) for 6 h, washed twice with PBS, incubated with DCFDA dye (15 μM) for 40 min at 37 °C, and finally fluorescence intensity was read using with a fluorometric plate reader (Spectramax, Gemini EM) at excitation and emission wavelengths of 485 and 528 nm, respectively.

### 2.8. Lipid peroxidation

Lipid peroxidation assay was done using Cayman's Chemicals Kit (USA) according to the manufacturer's protocols reported previously (Sharma, Anderson, and Dhawan, 2012). Briefly, the cells exposed to SeNRs (IC<sub>50</sub> concentration) for 6 h were harvested, washed with PBS, and centrifuged at 4 °C for 6 min at 1,500 rpm. Then, cell pellet was sonicated (15 W, 10 s) to obtain the cell lysate. Ferrous ions were then added to the cell extract, which following a reaction with lipid hydroperoxide resulted in the formation of ferric ions. The formation of ferric ions was detected spectrophotometrically at 500 nm using thiocyanate ion as the chromogen on a microplate reader (Bio-Tek, Winooski, USA).

## 2.9. Mitochondrial membrane potential (MMP) assessment

MMP values were detected using the fluorescent probe 5,5',6,6'-tetrachloro-1,1',3,3'-tetraethylbenzimidazolcarbocyanine iodide (JC-1; Sigma-Aldrich, USA) based on the protocol reported previously (Sharma, Anderson, and Dhawan, 2012). Briefly, cells were exposed to SeNRs (IC<sub>50</sub> concentration) for 24 h, harvested, and washed, incubated with 10 μM JC-1 for 15 min at 37 °C, washed, and re-suspended in PBS at a density of 10<sup>6</sup> cells/mL. The overall fluorescence was read using a fluorometric plate reader (Spectramax, Gemini EM) at excitation and emission wavelengths (green fluorescence, 485 nm and 535 nm) and (Red fluorescence, 550 nm and 600 nm), respectively.

## 2.10. Caspases activity assay

The cells exposed to SeNRs (IC<sub>50</sub> concentration) for 24 h were harvested, washed with PBS, and centrifuged at 4 °C for 6 min at 1,500 rpm. The cell pellet was then sonicated (15 W, 10 s) to obtain the cell lysate. Aliquots of cell extracts were used for the determination of the activity of caspase-3, caspase-8 and caspase-9 by Activity Assay Kits (Beyotime Biotechnology, Shanghai, China) following the manufacturer's protocols.

## 2.11. Real-time quantitative PCR analysis

Real-time quantitative PCR analysis for the determination of apoptotic gene expression was performed using an RG-3000 Real-Time Thermal Cycler (Corbett Research, Sydney, Australia). Briefly, the cells were treated with SeNRs (IC<sub>50</sub> concentration) for 24 h, harvested, and exposed to RNA extraction using a TRI reagent (Invitrogen, Carlsbad, CA, USA). The cDNA was then synthesized using 2 μg of total RNA with a Revert Aid™ First Strand cDNA Synthesis Kits (Fermentas, Germany) as per the manufacturer's protocol. The expression levels of Bax, Bcl-2, caspase-3, caspase-9, caspase-8, PI3K, Akt, mTOR, and β-actin were evaluated using gene-specific SYBR Green-based QuantiTect® Primer assays (Qiagen, Germany). The remaining products and primer sequences were done/used based on the previous reports (Li et al., 2015; Yang et al., 2016; Han et al., 2019; Wu et al., 2022).

## 2.12. ELISA assay

Cells treated with SeNRs NPs (IC<sub>50</sub> concentration) for 24 h, were pelleted and lysed using Cell Lysis Reagent (Sigma-Aldrich, USA) supplemented with protease inhibitor cocktail. The total protein concentration was then determined by the Bradford approach (He, 2011). The quantities of AKT, PI3K, and mTOR were then determined using relevant ELISA kits (Invitrogen, USA) as per the manufacturer's protocol.

## 2.13. Statistical analysis

Data was reported as the mean ± SD of three replicates and analyzed by one-way analysis of variance (ANOVA) with the Dunnett post hoc test using SPSS software (SPSS Inc., Chicago, IL, USA). *p* < 0.05 was considered significant.

## 3. Result and discussion

### 3.1. Characterization of synthesized SeNRs via ultrasonic-assisted hydrothermal method

Fig. 1A shows the FTIR spectrum of synthesized SeNRs. In the FTIR spectrum, two medium band intensities appeared at 464 cm<sup>-1</sup> and 660 cm<sup>-1</sup>, which are associated with bending vibrations of the Se–O bond. A broad and strong intensity peak was observed at 1130 cm<sup>-1</sup> derived from the stretching vibration of Se–O<sub>2</sub> (Refat and Elsbawy, 2011; Kannan et al., 2014). The FTIR spectrum of synthesized SeNRs is almost identical to that of Se nanostructures prepared with the assistance of biomolecule reported previously (Kannan et al., 2014).

The optical characteristics of SeNRs were detected by UV–vis spectrum analysis. The UV–vis spectrum of SeNRs is demonstrated in Fig. 1B. As it can be observed, a sharp maximum absorption (λ<sub>max</sub>) peak was observed at 298 nm, which revealed the formation of SeNRs inside the colloidal solution (Velayati et al., 2021). The SPR is derived from oscillation of conduction electrons following the excitation of nanostructure at a particular wavelength. The obtained data is in good agreement with the results reported by Velayati et al. who revealed a UV–vis absorption maximum of around 298 nm during the biosynthesis

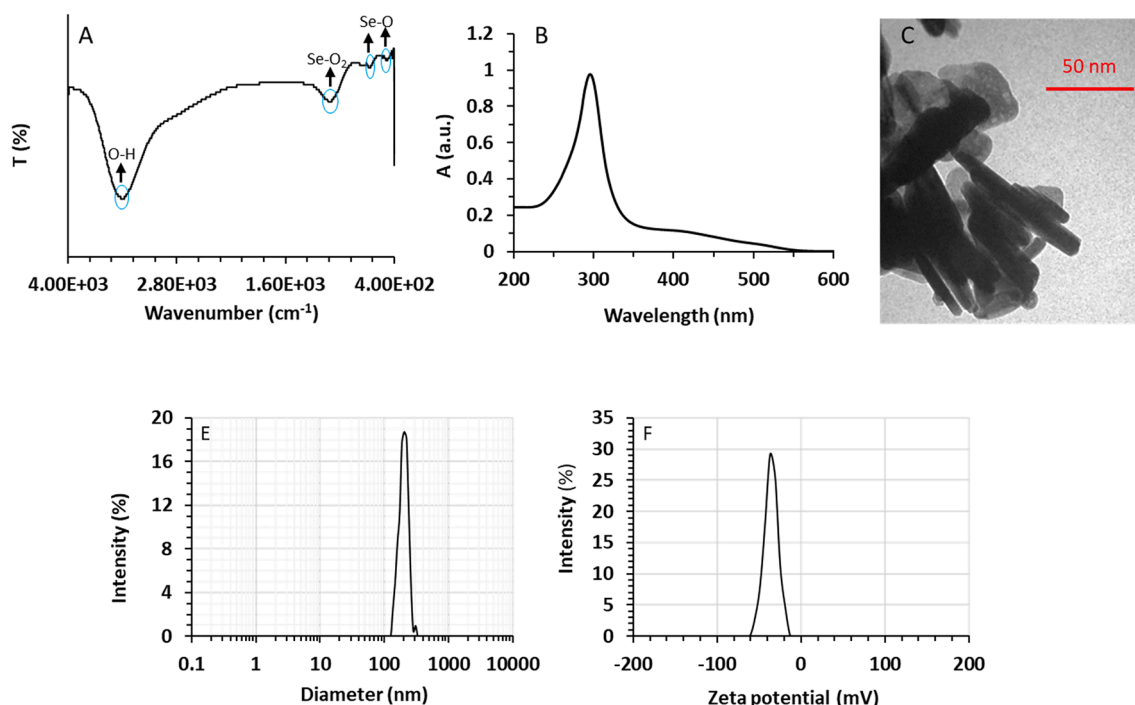


Fig. 1. Characterization of synthesized SeNRs by FTIR (A), UV–visible (B), TEM (C), DLS (D), and Zeta potential (E) methods.

of SeNRs using Gum Arabic (Velayati et al., 2021). Jiang et al. (Jiang, Cai, and Tan, 2017) showed that synthesis and optical characteristics of Se nanocrystals and NRs mediated by glycerin and glucose are heavily dependent on the incubation temperature and time. They reported that the  $\lambda_{\max}$  values of Se nanostructures prepared at different temperatures of 60 °C, 80 °C, 100 °C for 30 min and 120 °C with aging for 45 days were around 290 nm, 380 nm, 510 nm, and 630 nm, respectively (Jiang, Cai, and Tan, 2017). The detected localized SPR at  $\lambda_{\max}$  of 298 nm can be associated with the reduction of Se ions to Se atoms in the colloidal solution which might result in the appearance of SeNRs with a small size and homogenous morphology (Velayati et al., 2021). The shifting of the  $\lambda_{\max}$  value of NRs is related to the formation and size of these nanostructures (Jiang, Cai, and Tan, 2017; Velayati et al., 2021). Based on these facts, the sharp peak detected in the spectrum of SeNRs can be assigned to the tiny sizes and narrow distribution of synthesized nanostructures (Jiang, Cai, and Tan, 2017; Velayati et al., 2021).

As a consequence, it was confirmed that the ultrasonic-assisted hydrothermal method provides small-sized SeNRs with dispersed NR morphology.

TEM analysis also was done to determine the diameter and morphology of synthesized SeNRs. According to the TEM image, Se nanostructures had a rod-shaped morphology (Fig. 1C). Also, it was determined that SeNRs had lengths ranging from 50 to 100 nm with a diameter of around 10 nm. The obtained data confirm the TEM data of other studies such as Velayati et al. (Velayati et al., 2021) and Fresneda et al. (Fresneda et al., 2018) that reported the biosynthesis of SeNRs with an average size of less than 50 nm. However, Cao et al. reported that SeNRs synthesized at 130 °C by CTAB-assisted hydrothermal approach had sizes ranging from 60 to 80 nm and lengths of several micrometers (Cao et al., 2011). These variations in reported data could be related to differences in the precursor salt, temperature, pH, incubation time, and assistance of sonication (Tuyen et al., 2023; Zhang et al., 2023).

Moreover, DLS data displayed that SeNRs are well-dispersed with an average size of 204.68 nm (Fig. 1D). The differences in the obtained size of SeNRs using DLS and TEM characterization techniques could be based on the dissimilar principles and detection principles (Gholami-Shabani et al., 2023). The probable stability of synthesized SeNRs was assessed by zeta potential measurement. The zeta potential value can be appointed as an important indicator of the nanostructure stability and relevant dispersion (Gholami-Shabani et al., 2023). Synthesized SeNRs via ultrasonic-assisted hydrothermal method displayed a zeta potential value of  $-37.29$  mV (Fig. 1E), indicating that these NRs have a negatively-charged surface, which results in good colloidal stability of SeNRs. Because of electrostatic repulsion between similar charges could inhibit nanoparticle aggregation and induce long term stability (Gholami-Shabani et al., 2023).

### 3.2. Toxicity of SeNRs to normal and cancer cells

Cancer can develop when the balance between cell division and apoptosis is perturbed (Heiden et al., 2009). As a result, inhibition of cell proliferation can be appointed as a promising way of inhibiting cancer progression. In the first step, we aimed to show that SeNRs could selectively reduce the proliferation of DU-145 prostate cancer cells relative to the human prostate normal cell line, RWPE-1. As shown in Fig. 2A, SeNRs were able to inhibit the proliferation of both cancer and normal cells, however, the anti-proliferative effects of SeNRs against DU-145 prostate cancer cells were more significant than normal prostate cells. The half-maximal inhibitory ( $IC_{50}$ ) concentration of SeNRs against DU-145 prostate cancer cells and prostate normal cell line, RWPE-1 were calculated to be about 2.95  $\mu\text{g}/\text{mL}$  and 50.06  $\mu\text{g}/\text{mL}$ , respectively, at 24 h.

We detected that following the incubation of cells with SeNRs, the inhibition rate of DU-145 cells augmented in a concentration-dependent manner, whereas the cell viability of RWPE-1 cells was not influenced under the same concentration up to 10  $\mu\text{g}/\text{mL}$  of SeNRs. Thus, these data exhibited that SeNRs were nontoxic against normal cells and triggered selective antitumor activities. Kong et al. reported that the inhibitory rate of Se nanoparticles (10–30 nm) against androgen-independent DU-145 prostate cancer cell was higher than that of androgen-dependent LNCaP cells (Kong et al., 2011). Also, they revealed that Se nanoparticles inhibited prostate cancer cell growth after 48 h treatment, at a higher rate than 24 h treatment (Kong et al., 2011). Sonkusre et al. (Sonkusre, 2020) reported that the Se nanoparticles with a size of  $>100$  nm were able to inhibit the proliferation of metastatic prostate cancer cells down to 60 % at a concentration of 6  $\mu\text{g}/\text{mL}$  after 24 h.

Overall, the literature survey of  $IC_{50}$  concentration values of se-based nanostructures against various cancer cell types (Table 1) implied that the synthesized SeNRs using the ultrasonic-assisted hydrothermal method might have a strong anticancer activity.

To further investigate whether synthesized SeNRs induced selective cell cytotoxicity, DU-145 prostate cancer cells and human prostate normal cell line, RWPE-1, were treated with  $IC_{50}$  concentration of SeNRs (2.95  $\mu\text{g}/\text{mL}$ ) for 24 h, and cell cytotoxicity was assessed by the well-known LDH leakage assay. Interestingly, SeNRs were toxic to DU-145 prostate cancer cells, whereas no significant LDH release was detected in SeNRs-treated normal cell line (Fig. 2B). These results might suggest that SeNRs serve as an effective antitumor nanostructure that can damage cancer cell membranes, as a similar mechanism has been reported previously upon the interaction of biogenic Se nanoparticles with prostate cancer cells (Sonkusre, 2020; Sonkusre and Cameotra, 2017). It has been also shown that Se nanostructures ( $\sim 20$  nm) might trigger cytotoxicity in the human breast and liver cancer cell lines through the induction of membrane leakage (Alkudhry et al., 2020). Also, Acharya et al. (Acharya, Nithyananthan, and Thirunavukkarasu, 2023)

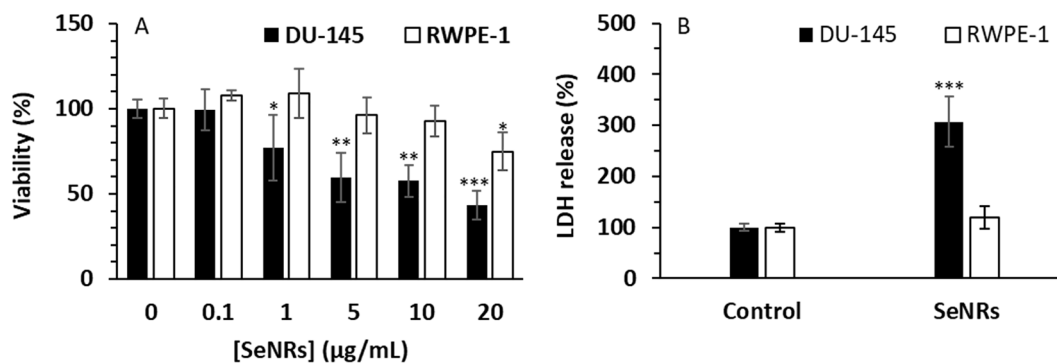


Fig. 2. Assessment of cell viability (A) and membrane leakage (B) in DU-145 prostate cancer cells and prostate normal cell line, RWPE-1, after incubation with different concentrations of SeNRs for MTT assay and  $IC_{50}$  concentration of SeNRs for LDH assay for 24 h. Data are shown as mean  $\pm$  SD ( $n = 3$ ). \* $p < 0.05$ , \*\* $p < 0.01$ , \*\*\* $p < 0.001$  relative to control.

**Table 1**

The comparison of IC<sub>50</sub> values of Se nanostructures against different cancer cell lines determined previously.

Se nanostructure	Size (nm)	Synthesis approach	Cell line	IC <sub>50</sub>	Ref.
Spherical	52.5	Green synthesis	MDA-MB-231 triple-negative breast cancer cells	34 µg/mL	(Cittrarasu et al., 2021)
Spherical	45–90	Green synthesis	A549 lung cancer cells	25 µg/mL	(Alagesan and Venugopal, 2019)
Spherical	20–50	Green synthesis	A549 lung cancer cells	3 µg/mL	(Bharathi et al., 2020)
NRs	24	Green synthesis	CT26 colon carcinoma cell line	1453 µg/mL	(Velayati et al., 2021)
NRs	10	Ultrasonic-assisted hydrothermal method	DU-145 prostate cancer cell line	2.95 µg/mL	This work

reported that membrane leakage of cancer cells could be one of the main possible mechanisms that Se nanoparticles with a size of ~80 nm and an IC<sub>50</sub> concentration of 5 µg/mL can induce anticancer activity in liver cancer cells.

### 3.3. SeNRs induced oxidative stress in DU-145 cells

Oxidative stress and associated ROS formation and lipid peroxidation have been reported to be the main mechanism in Se particles-induced cytotoxicity (Liu et al., 2015; Menon et al., 2018; Saranya et al., 2023). Many nanoparticles have stimulated cell death, through the generation of intracellular ROS and lipid peroxidation (Alavi and Yarani, 2023; Othman et al., 2022). Thus, ROS generation can be ascribed as a key cellular process triggered by nanostructures which could lead to cell death (Menon et al., 2018).

In agreement with previous studies (Menon et al., 2018; Othman et al., 2022), we observed that the DU-145 prostate cancer cells exposed to SeNRs (2.95 µg/mL) for 6 h demonstrated a significant ( $***p < 0.001$ ) elevation in the ROS generation. This was evident by a significant increase in the DCF fluorescence intensity when determined quantitatively (Fig. 3A).

A lipid peroxidation assay was done to determine the formation of lipid peroxidation by-products. A statistically significant ( $**p < 0.01$ ) increase in lipid peroxidation was detected (at 2.95 µg/mL) in DU-145 prostate cancer cells after 6 h exposure to SeNRs (Fig. 3B). Although SeNRs with a concentration of 2.95 µg/mL after 6 h induced significant oxidative stress in the human prostate normal cell line, RWPE-1, this effect was more pronounced in DU-145 prostate cancer cells relative to

noncancerous cells.

The anticancer mechanism of Se is still arguable, however, Se could facilitate the proliferation of normal cells while mitigating the growth of tumor cells (Menon et al., 2018). The Se particle mechanism of action is heavily assigned to the selective and remarkable Se accumulation, which results in an apparent increase in ROS generation in tumor cells, but not in noncancerous tissues (Kumar, Tomar, and Acharya, 2015; Menon et al., 2018). Wang et al. (Wang et al., 2015) reported that the selective distribution of Se particles in tumor cells and not in noncancerous tissues did not stimulate any significant host cytotoxicity, but resulted in ROS burst in tumor cells and apparent suppressive activity on cancer cell growth, which is in good agreement with the data reported in this study.

### 3.4. SeNRs induced apoptosis through the intrinsic signaling pathway in DU-145 cells

Several mechanisms have been reported to exemplify the anticancer function of Se nanostructure, which comprise initiation of cell apoptosis, control of cell proliferation, regulation of oxidative stress, trigger of the immune system, and inhibition of metastasis and invasion (Menon et al., 2018). Among these effective anticancer activities of Se nanostructures, apoptosis received the most consideration and has been indicated to be the basic strategy for cancer therapy by seleno compounds (Menon et al., 2018).

Se nanoparticles can stimulate oxidative stress, a critical cellular event that leads to cell apoptosis (Menon et al., 2018). Apoptosis can either occur through extrinsic or intrinsic pathways, where, the death receptor, which is present on the cell membrane, can interact with proapoptotic compounds to initiate the extrinsic pathway through the caspase-8 activation. In contrast, the intrinsic pathway is triggered by the activation of caspase-9 due to DNA damage or other forms of cell stress (Hongmei, 2012; Sahoo et al., 2023). The potent approach for cancer therapy is based on triggering DNA damage thus, the anti-cancer activity of Se nanoparticles can be typically allocated to their capabilities to generate excessive levels of ROS that lead to DNA damage and thereby apoptosis induction (Menon et al., 2018).

Zhao et al, showed that the selenium nanostructures might be able to induce p53 expression in cancer cells resulting in the upregulation of caspase-9, reduction of MMP, and induction of apoptosis (Zhao et al., 2017). Therefore, the anticancer compound-stimulated mitochondrial intrinsic pathway of apoptosis depends on the MMP collapse and alteration of the Bax/Bcl-2 ratio, with a concomitant upregulation in Bax expression and downregulation in Bcl-2 expression (Brunelle and Letai, 2009).

Therefore, we first investigated if the apparent selective anticancer activity of synthesized SeNRs could be related to a MMP loss. Our data showed that SeNRs induced a significant drop ( $***p < 0.001$ ) in MMP values at 24 h in DU-145 prostate cancer cells, which was not pronounced in normal cells (Fig. 4A).

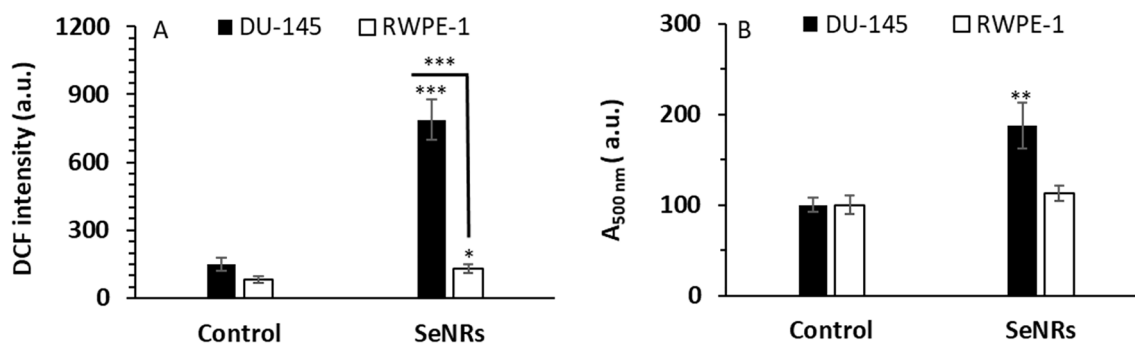


**Fig. 3.** Assessment of ROS generation (A) and lipid peroxidation (B) in DU-145 prostate cancer cells and prostate normal cell line, RWPE-1, after incubation with IC<sub>50</sub> concentration of SeNRs for 6 h. Data are shown as mean ± SD (n = 3). \*p < 0.05, \*\*p < 0.01, \*\*\*p < 0.001 relative to control.

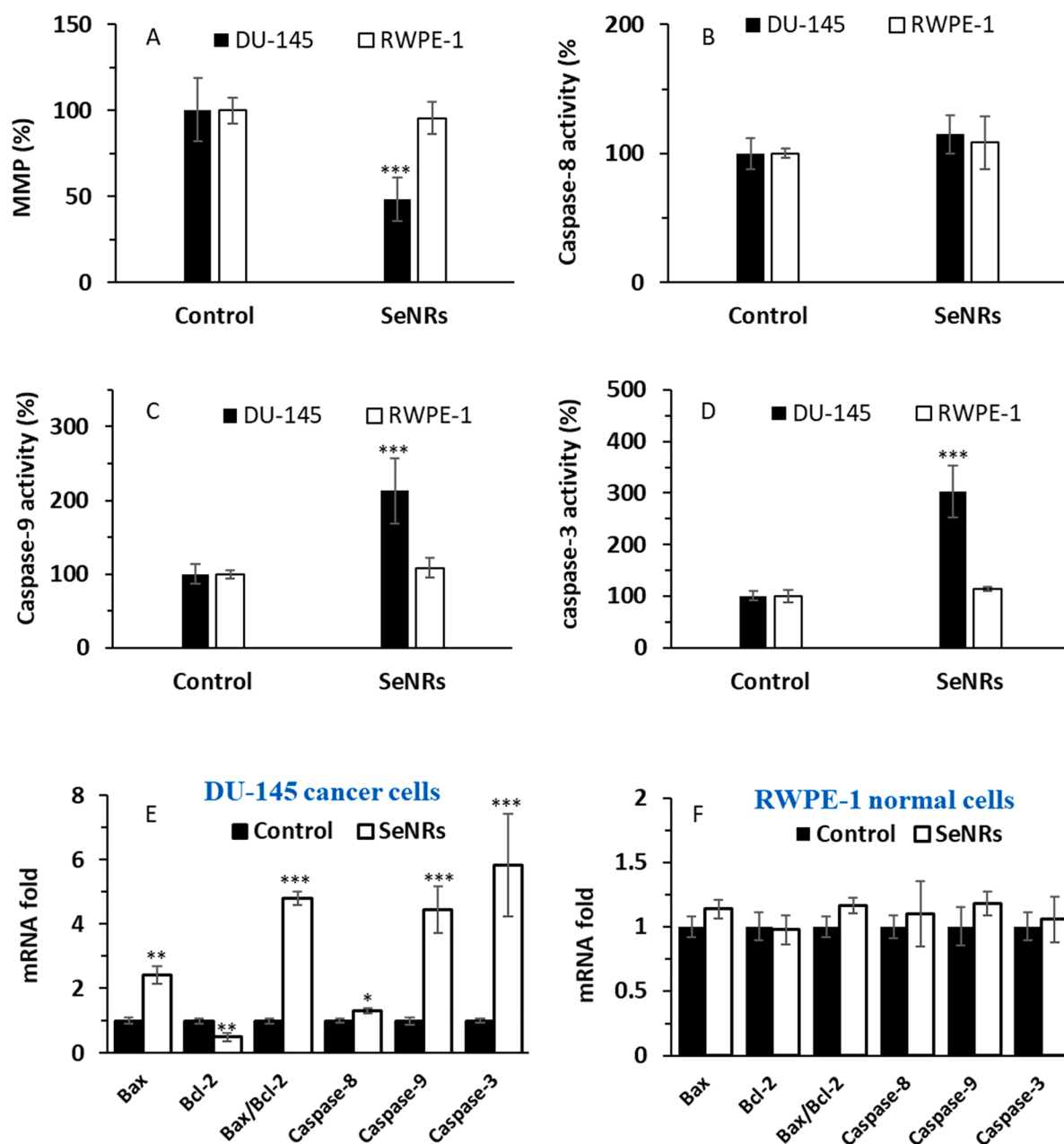


**Fig. 4.** Assessment of MMP loss (A), caspase-8 activity (B), caspase-9 activity (C), and caspase-3 activity (D) in DU-145 prostate cancer cells and prostate normal cell line, RWPE-1, after incubation with  $IC_{50}$  concentration of SeNRs for 24 h. mRNA fold in DU-145 prostate cancer cells (E) and mRNA fold in a prostate normal cell line, RWPE-1 (F), after incubation with  $IC_{50}$  concentration of SeNRs for 24 h. Data are shown as mean  $\pm$  SD (n = 3). \*p < 0.05, \*\*p < 0.01, \*\*\*p < 0.001 relative to control.

We then performed caspase-8 (Fig. 4B), caspase-9 (Fig. 4C) and caspase-3 (Fig. 4D) activity assays in both cancer and normal cells after exposure to 2.95  $\mu$ g/mL SeNRs at 24 h. It was deduced that at 24 h, caspase-9 (Fig. 4C) and caspase-3 (Fig. 4D) activities differ significantly in comparison with control samples in DU-145 prostate cancer cells, however, SeNRs were not able to trigger a significant increase in caspase activity in the human prostate normal cell line, RWPE-1. It was revealed caspase-8 activity differed slightly relative to control samples, following exposure of DU-145 prostate cancer cells to 2.95  $\mu$ g/mL SeNRs at 24 h (Fig. 4B).

The same trend was also observed when we studied caspase-8, -9 and -3 mRNA expression in both cancer (Fig. 4E) and normal cells (Fig. 4F) after incubation with 2.95  $\mu$ g/mL SeNRs at 24 h. Although the caspase-8 mRNA expression increased in DU-145 prostate cancer cells relative to the control group, this increase was less pronounced than

overexpression of caspase-9 and caspase-3 mRNA.

We then investigated the role of proapoptotic (Bax mRNA) and antiapoptotic (Bcl-2 mRNA) members associated with mitochondrial regulation during apoptosis (Brunelle and Letai, 2009). Generally, the MMP loss could be connected with an increase in Bax/Bcl-2 ratio. At 24 h, Bax mRNA upregulated significantly in cancer cells relative to the control sample. Moreover, we detected a significant reduction between SeNRs-incubated cancer cells and controls for Bcl-2 mRNA expression in DU-145 prostate cancer cells at 24 h. Our data indicated that SeNRs could lead to a significant multiplication in the Bax/Bcl-2 ratio at 24 h in cancer cells (Fig. 4E), whereas this ratio was not significantly changed in normal cells relative to the control sample (Fig. 4F).

These outcomes designated that SeNRs selectively induce apoptosis through ROS-associated mitochondrial dysfunction in the human prostate cancer cells and slightly through the extrinsic death receptor

pathway, which is in good agreement with the study reported by Zhao et al. (Zhao et al., 2017). Zhang et al. (Zhang et al., 2013) also reported that Se nanoparticles in combination with ATP could trigger cancer cell apoptosis through the mitochondrial-mediated pathway, revealed by the overactivation of caspase-3,-8 and -9. Furthermore, Yu et al. (Yu et al., 2016) and Zheng et al. (Zheng et al., 2012) reported that PEGylated Se nanostructures had anticancer activities through DNA damage and inhibition of cell proliferation mediated by mitochondrial fragmentation and apoptosis. Moreover, Chen et al. (Chen et al., 2008) demonstrated that Se nanoparticles biosynthesized in polysaccharide solutions trigger mitochondria-mediated apoptosis in human melanoma cells.

### 3.5. SeNRs inhibited the PI3K/AKT/mTOR signaling pathway in DU-145 cells

Recent reports have shown that prostate cancer cells can be controlled by the PI3K/AKT/mTOR signaling cascade (Li et al., 2018; Pungsrinont,Kallenbach,and Baniahmad, 2021). Yu et al. (Yu et al., 2022) reported that the proliferation and progression of prostate cancer cells occur following upregulation of the PI3K/AKT signaling pathway. Therefore, inhibition of the PI3K/AKT/mTOR signaling pathway can be used a potential strategy for the control of prostate cancer cell proliferation.

Hence, the expression levels of PI3K, AKT, and mTOR mRNA and proteins were detected after 24 h incubation of DU-145 prostate cancer cells with 2.95  $\mu\text{g}/\text{mL}$  SeNRs. As shown in Fig. 5, SeNR incubation caused an apparent decrease in the PI3K, Akt, and mTOR mRNA of DU-145 cells (Fig. 5A) and restrained the levels of AKT, PI3K, and mTOR proteins, compared to the control group (Fig. 5B). In addition, pre-treatment of DU-145 prostate cancer cells with 10  $\mu\text{M}$  LY294002 for 2 h and addition of 2.95  $\mu\text{g}/\text{mL}$  SeNRs for 24 h further reduced the levels

of PI3K, Akt, and mTOR proteins and relevant cell viability relative to SeNRs-treated cells (Fig. 5B and C). Therefore, these data indicated that the synthesized SeNRs downregulated the PI3K/Akt/mTOR signaling pathway.

Previous results have shown that Se nanoparticles can induce apoptotic effects in prostate cancer cells through Akt-mediated signaling pathways (Kong et al., 2011). Also, Wang et al. (Wang et al., 2022) reported that biosynthesized Se nanoparticles could stimulate apoptosis and autophagy in gastric cancer cells by inhibiting the PI3K/Akt/mTOR signaling pathway. Furthermore, Guo et al. (Guo et al., 2017) indicated that modification of Se nanoparticles with curcumin could stimulate liver cancer cell apoptosis through oxidative stress-mediated p53 and AKT signaling cascades. Additionally, Woo et al. (Woo et al., 2021) revealed that Se particles could inhibit the proliferation of trastuzumab-resistant breast tumor cells via reduction of Akt expression.

## 4. Conclusion

In general, after the fabrication of SeNRs via the ultrasonic-assisted hydrothermal method, we explored the characteristics of these nanostructures. Then, the selective anticancer effects of SeNRs against prostate cancer DU-145 cells were investigated, whereas a human prostate normal cell line, RWPE-1, was used as a control. It was shown that Se nanostructures with a rod-shaped morphology with a diameter of around 10 nm had a potential selective anticancer activity on DU-145 prostate cancer cells by induction of membrane leakage, oxidative stress, intrinsic apoptosis, and targeting the PI3K/AKT/mTOR signaling pathway, while these particles were not toxic for normal prostate cells. Therefore, the synthesized SeNRs could be further evaluated *in vitro* and *in vivo* for use as nano-based systems in the treatment of prostate cancer.

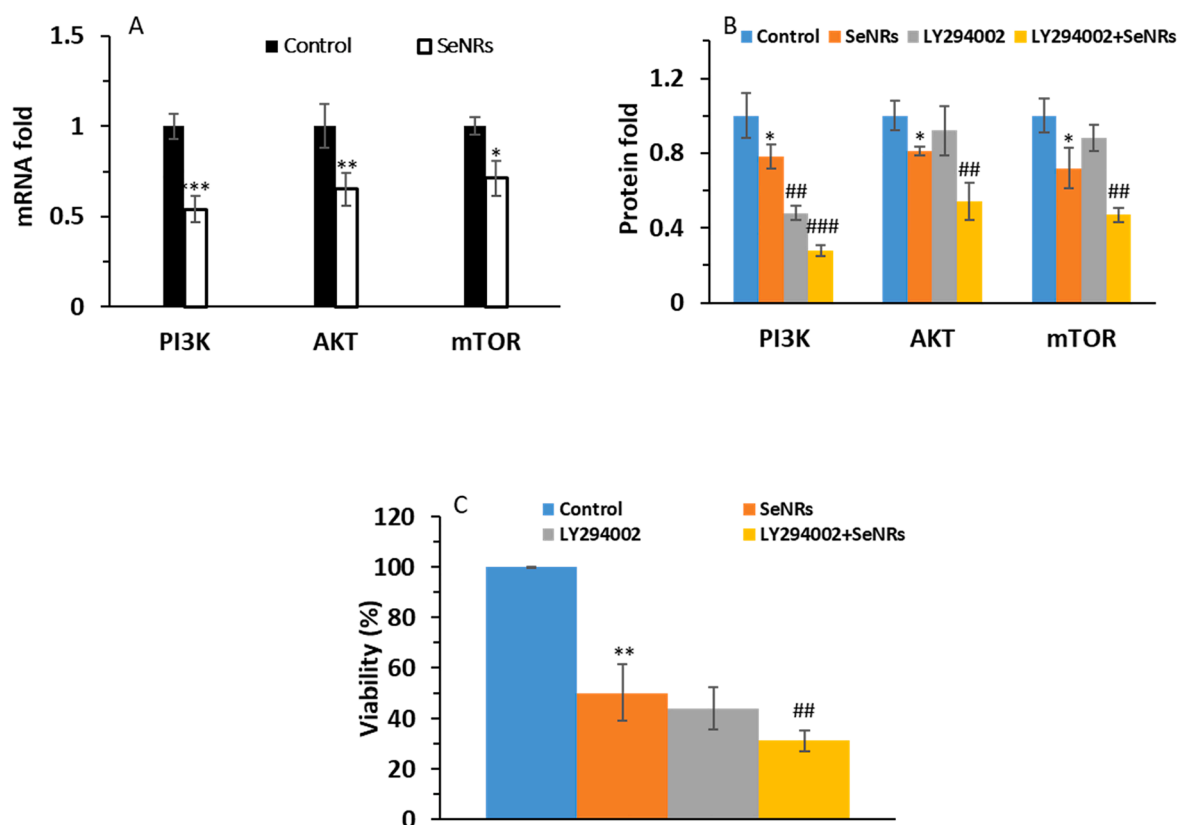


**Fig. 5.** Assessment of PI3K, Akt, and mTOR mRNA expression in DU-145 prostate cancer cells after incubation with  $\text{IC}_{50}$  concentration of SeNRs for 24 h (A). The expression levels of PI3K, Akt, and mTOR proteins (B) and cell viability (C) in DU-145 prostate cancer cells pre-treated with 10  $\mu\text{M}$  LY294002 for 2 h and the addition of  $\text{IC}_{50}$  concentration of SeNRs for 24 h. Data are shown as mean  $\pm$  SD (n = 3). \* $p$  < 0.05, \*\* $p$  < 0.01, \*\*\* $p$  < 0.001 relative to control. ## $p$  < 0.01 and ### $p$  < 0.001 relative to SeNP-treated group.

## CRedit authorship contribution statement

**Du Shen:** Conceptualization, Data curation, Writing – original draft, Writing – review & editing, Visualization, Investigation, Validation, Formal analysis, Methodology. **Shaosan Kang:** Conceptualization, Funding acquisition, Data curation, Writing – review & editing, Visualization, Investigation, Validation, Formal analysis, Methodology, Supervision, Resources, Project administration, Software.

## Declaration of competing interest

The authors declare that they have no known competing financial interests or personal relationships that could have appeared to influence the work reported in this paper.

## Acknowledgment

The technical support provided by all colleagues and students highly appreciated.

## References

- Acharya, S., Nithyananthan, S., Thirunavukkarasu, C., 2023. Selenium nanoparticles show anticancer activity through regulation of HIF-1 $\alpha$  and HIF-2 $\alpha$  under hypoxic condition in liver cancer cells. *DNA and Cell Biology*.
- Ahmad, Maged Sayed, Manal Mohamed Yasser, Essam Nageh Sholkamy, Ali Mohamed Ali, and Magda Mohamed Mehanni. 2015. 'Anticancer activity of biostabilized selenium nanorods synthesized by Streptomyces bikiniensis strain Ess amA-1', *International journal of nanomedicine*: 3389-401.
- Alagesan, V., Venugopal, S., 2019. Green synthesis of selenium nanoparticle using leaves extract of withania somnifera and its biological applications and photocatalytic activities. *Bionanoscience* 9, 105–116.
- Alavi, M., Yarani, R., 2023. ROS and RNS modulation: the main antimicrobial, anticancer, antidiabetic, and antineurodegenerative mechanisms of metal or metal oxide nanoparticles. *Nano Micro Biosystems* 2, 22–30.
- Alkudhairy, A.A., Wahab, R., Siddiqui, M.A., Ahmad, J., 2020. Selenium nanoparticles induce cytotoxicity and apoptosis in human breast cancer (MCF-7) and liver (HEPG2) cell lines. *Nanoscience and Nanotechnology Letters* 12, 324–330.
- Bharathi, S., Kumaran, S., Suresh, G., Ramesh, M., Thangamani, V., Pugazhendian, S.R., Sathiyamurthy, K., 2020. 'Extracellular synthesis of nanoselenium from fresh water bacteria bacillus sp., and its validation of antibacterial and cytotoxic potential', *biocatalysis and agricultural*. *Biotechnology* 27, 101655.
- Bisht, N., Phalswal, P., Khanna, P.K., 2022. Selenium nanoparticles: a review on synthesis and biomedical applications. *Materials Advances* 3, 1415–1431.
- Brunelle, J.K., Letai, A., 2009. Control of mitochondrial apoptosis by the Bcl-2 family. *Journal of Cell Science* 122, 437–441.
- Cao, G.S., Zhang, X.J., Ling, S.u., Ruan, Y.Y., 2011. Hydrothermal synthesis of selenium and tellurium nanorods. *Journal of Experimental Nanoscience* 6, 121–126.
- Chen, T., Wong, Y.-S., Zheng, W., Bai, Y., Huang, L., 2008. Selenium nanoparticles fabricated in undaria pinnatifida polysaccharide solutions induce mitochondria-mediated apoptosis in A375 human melanoma cells. *Colloids and Surfaces b: Biointerfaces* 67, 26–31.
- Chen, Y.-T., Zhang, W., Fan, Y.-Q., Xiao-qing, X.u., Zhang, Z.-X., 2006. Hydrothermal preparation of selenium nanorods. *Materials Chemistry and Physics* 98, 191–194.
- Citrarasu, V., Kaliannan, D., Dharmam, K., Maluventhen, V., Easwaran, M., Liu, W.C., Balasubramanian, B., Arumugam, M., 2021. Green synthesis of selenium nanoparticles mediated from *Cropegia bulbosa* roxb extract and its cytotoxicity, antimicrobial, mosquitocidal and photocatalytic activities. *Scientific Reports* 11, 1032.
- El-Fakharany, E.M., Abu-Serie, M.M., Ibrahim, A., Eltarahony, M., 2023. Anticancer activity of lactoferrin-coated biosynthesized selenium nanoparticles for combating different human cancer cells via mediating apoptotic effects. *Scientific Reports* 13, 9579.
- Fresneda, Miguel A. Ruiz, Josemaría Delgado Martín, Jaime Gómez Bolívar, María V. Fernández Cantos, Germán Bosch-Estévez, Marcos F. Martínez Moreno, and Mohamed L. Merroun. 2018. 'Green synthesis and biotransformation of amorphous Se nanospheres to trigonal 1D Se nanostructures: impact on Se mobility within the concept of radioactive waste disposal', *Environmental Science: Nano*, 5: 2103-16.
- Gao, X., Yao, Y., Chen, X., Lin, X., Yang, X., Ho, C.-T., Li, B., Chen, Z., 2022. Lentinan-functionalized selenium nanoparticles induce apoptosis and cell cycle arrest in human colon carcinoma HCT-116 cells. *Frontiers in Nutrition* 9, 987807.
- Gayathri, M.K., Esha, D.R., Thangavelu, S.L., Perumal, E., 2023. Green synthesis of curcumin and clove mediated selenium nanoparticles and its anticancer activity against osteosarcoma cell line. *Journal of Survey in Fisheries Sciences* 10, 300–311.
- Gholami-Shabani, M., Sotoodehnejadnematalahi, F., Shams-Ghahfarokhi, M., Eslamifar, A., Razzaghi-Abyaneh, M., 2023. Platinum nanoparticles as potent anticancer and antimicrobial agent: green synthesis, physical characterization, and in-vitro biological activity. *Journal of Cluster Science* 34, 501–516.
- Guo, M., Li, Y., Lin, Z., Zhao, M., Xiao, M., Wang, C., Tiantian, X.u., Xia, Y.u., Zhu, B., 2017. Surface decoration of selenium nanoparticles with curcumin induced HepG2 cell apoptosis through ROS mediated p53 and AKT signaling pathways. *RSC Advances* 7, 52456–52464.
- Han, Y., Ming, L.u., Zhou, J., 2019. Bufenin IIb induces androgen-independent prostate cancer cells apoptosis through p53 pathway in vitro. *Toxicol* 168, 16–21.
- Hasannia, M., Abnous, K., Taghdisi, S.M., Nekooei, S., Ramezani, M., Alibolandi, M., 2022. Synthesis of doxorubicin-loaded peptosomes hybridized with gold nanorod for targeted drug delivery and CT imaging of metastatic breast cancer. *Journal of Nanobiotechnology* 20, 1–27.
- Hauk, T.S., Jennings, T.L., Tetyana Yatsenko, J., Kumaradas, C., Chan, W.C.W., 2008. Enhancing the toxicity of cancer chemotherapeutics with gold nanorod hyperthermia. *Advanced Materials* 20, 3832–3838.
- He, F., 2011. Bradford protein assay. *Bio-Protocol* e45.
- Heiden, V., Matthew, G., Cantley, L.C., Thompson, C.B., 2009. Understanding the Warburg effect: the metabolic requirements of cell proliferation. *Science* 324, 1029–1033.
- Hongmei, Zhao. 2012. 'Extrinsic and intrinsic apoptosis signal pathway review.' in, *Apoptosis and medicine (InTechOpen)*.
- Jiang, F., Cai, W., Tan, G., 2017. Facile synthesis and optical properties of small selenium nanocrystals and nanorods. *Nanoscale Research Letters* 12, 1–6.
- Kang, S., Yim, G., Chae, S.-Y., Kim, S., Gil, Y.-G., Kim, Y.-K., Min, D.-H., Jang, H., 2022. Rhodium–Tellurium nanorod synthesis using galvanic replacement-polyol regrowth for thermo-dynamic dual-modal cancer phototherapy. *ACS Applied Materials & Interfaces* 14, 40513–40521.
- Kannan, S., Mohanraj, K., Prabhu, K., Barathan, S., Sivakumar, G., 2014. Synthesis of selenium nanorods with assistance of biomolecule. *Bulletin of Materials Science* 37, 1631–1635.
- Kong, L., Yuan, Q., Zhu, H., Li, Y., Guo, Q., Wang, Q., Bi, X., Gao, X., 2011. The suppression of prostate LNCaP cancer cells growth by selenium nanoparticles through Akt/Mdm2/AR controlled apoptosis. *Biomaterials* 32, 6515–6522.
- Kuchibhatla, S.V.N.T., Karakoti, A.S., Bera, D., Seal, S., 2007. One dimensional nanostructured materials. *Progress in Materials Science* 52, 699–913.
- Kumar, S., Tomar, M.S., Acharya, A., 2015. Carboxylic group-induced synthesis and characterization of selenium nanoparticles and its anti-tumor potential on Dalton's lymphoma cells. *Colloids and Surfaces b: Biointerfaces* 126, 546–552.
- Li, J., Lai, Y., Cao, Y.i., Tao, D.u., Zeng, L., Wang, G., Chen, X., Chen, J., Yongsheng, Y.u., Zhang, S., 2015. SHARPIN overexpression induces tumorigenesis in human prostate cancer LNCaP, DU145 and PC-3 cells via NF-KB/ERK/AKT signaling pathway. *Medical Oncology* 32, 1–9.
- Li, X., Tang, Y., Fangmiao, Y.u., Sun, Y.u., Huang, F., Chen, Y., Yang, Z., Ding, G., 2018. Inhibition of prostate cancer DU-145 cells proliferation by anthopleura juncea oligopeptide (YVPGP) via PI3K/AKT/mTOR signaling pathway. *Marine Drugs* 16, 325.
- Liao, JinFeng, Li, WenTing, Peng, JinRong, Yang, Q., Li, H.e., Wei, YuQuan, Zhang, XiaoNing, Qian, ZhiYong, 2015. Combined cancer photothermal-chemotherapy based on doxorubicin/gold nanorod-loaded polymersomes. *Theranostics* 5, 345.
- Liu, T., Zeng, L., Jiang, W., Yuanting, F.u., Zheng, W., Chen, T., 2015. 'Rational design of cancer-targeted selenium nanoparticles to antagonize multidrug resistance in cancer cells', *nanomedicine: nanotechnology. Biology and Medicine* 11, 947–958.
- Ma, Y., Lin, Y., Xiao, X., Zhou, X., Li, X., 2006. Sonication–hydrothermal combination technique for the synthesis of titanate nanotubes from commercially available precursors. *Materials Research Bulletin* 41, 237–243.
- Menon, S., Ks, S.D., Santhiya, R., Rajeshkumar, S., Kumar, V., 2018. Selenium nanoparticles: a potent chemotherapeutic agent and an elucidation of its mechanism. *Colloids and Surfaces b: Biointerfaces* 170, 280–292.
- Othman, M.S., Obeidat, S.T., Al-Bagawi, A.H., Fareid, M.A., Fehaid, A., Abdel Moneim, A.E., 2022. Green-synthesized selenium nanoparticles using berberine as a promising anticancer agent. *Journal of Integrative Medicine* 20, 65–72.
- Polivka Jr, J., Janku, F., 2014. Molecular targets for cancer therapy in the PI3K/AKT/mTOR pathway. *Pharmacology & Therapeutics* 142, 164–175.
- Pungsrinont, T., Kallenbach, J., Banihmad, A., 2021. Role of PI3K-AKT-mTOR pathway as a pro-survival signaling and resistance-mediating mechanism to therapy of prostate cancer. *International Journal of Molecular Sciences* 22, 11088.
- Rayman, M.P., 2012. Selenium and human health. *The Lancet* 379, 1256–1268.
- Refat, M.S., Elsabay, K.M., 2011. Infrared spectra, raman laser, XRD, DSC/TGA and SEM investigations on the preparations of selenium metal, (sb 2 O 3, ga 2 O 3, SnO and HgO) oxides and lead carbonate with pure grade using acetamide precursors. *Bulletin of Materials Science* 34, 873–881.
- Sahoo, G., Samal, D., Khandayataray, P., Murthy, M.K., 2023. A review on caspases: key regulators of biological activities and apoptosis. *Molecular Neurobiology* 1–33.
- Saranya, T., Ramya, S., Kavitha, K., Paulpandi, M., Cheon, Y.-P., Winster, S.H., Balachandar, V., Narayanasamy, A., 2023. Green synthesis of selenium nanoparticles using solanum nigrum fruit extract and its anti-cancer efficacy against triple negative breast cancer. *Journal of Cluster Science* 34, 1709–1719.
- Sharma, V., Anderson, D., Dhawan, A., 2012. Zinc oxide nanoparticles induce oxidative DNA damage and ROS-triggered mitochondria mediated apoptosis in human liver cells (HepG2). *Apoptosis* 17, 852–870.
- Shin, J., Kang, N., Kim, B., Hong, H., Le, Y.u., Kim, J., Kang, H., Kim, J.S., 2023. One-dimensional nanomaterials for cancer therapy and diagnosis. *Chemical Society Reviews*.
- Shukla, N., Singh, B., Kim, H.-J., Park, M.-H., Kim, K., 2020. Combinational chemotherapy and photothermal therapy using a gold nanorod platform for cancer treatment. *Particle & Particle Systems Characterization* 37, 2000099.

- Sonkusre, P., 2020. Specificity of biogenic selenium nanoparticles for prostate cancer therapy with reduced risk of toxicity: an in vitro and in vivo study. *Frontiers in Oncology* 9, 1541.
- Sonkusre, P., Cameotra, S.S., 2017. Biogenic selenium nanoparticles induce ROS-mediated necroptosis in PC-3 cancer cells through TNF activation. *Journal of Nanobiotechnology* 15, 1–12.
- Tuyen, Nguyen Ngoc Kim, Vo Khac Huy, Nguyen Huu Duy, Hoang An, Nguyen Thanh Hoai Nam, Nguyen Minh Dat, Quach Thi Thanh Huong, Nguyen Le Phuong Trang, Nguyen Do Phuong Anh, and Lu Thi Mong Thy. 2023. 'Green synthesis of selenium nanorods using Muntigia calabura leaf extract: Effect of pH on characterization and bioactivities'.
- ur Rehman, Khalil, Umber Zaman, Shahid Ullah Khan, Kamran Tahir, Bibi Hajira, Jehan Y Al-Humaidi, Moamen S Refat, Noor Saeed Khattak, and Dilfaraz Khan. 2023. 'Hydrothermal assisted eco-benign synthesis of novel  $\beta$ -galactosidase mediated Titanium dioxide nanoparticles ( $\beta$ -gal-TiO<sub>2</sub> NPs): Ultra efficient nanocatalyst for methylene blue degradation, inactivation of bacteria, and stabilization of DPPH radicals', *Materials Chemistry and Physics*, 294: 126877.
- Velayati, M., Hassani, H., Sabouri, Z., Mostafapour, A., Darroudi, M., 2021. Biosynthesis of se-nanorods using gum arabic (GA) and investigation of their photocatalytic and cytotoxicity effects. *Inorganic Chemistry Communications* 128, 108589.
- Wang, Y., Chen, P., Zhao, G., Sun, K., Li, D., Wan, X., Zhang, J., 2015. Inverse relationship between elemental selenium nanoparticle size and inhibition of cancer cell growth in vitro and in vivo. *Food and Chemical Toxicology* 85, 71–77.
- Wang, R., Ha, K.-Y., Dhandapani, S., Kim, Y.-J., 2022. Biologically synthesized black ginger-selenium nanoparticle induces apoptosis and autophagy of AGS gastric cancer cells by suppressing the PI3K/Akt/mTOR signaling pathway. *Journal of Nanobiotechnology* 20, 1–20.
- Woo, J., Kim, J.B., Cho, T., Yoo, E.H., Moon, B.-I., Kwon, H., Lim, W., 2021. Selenium inhibits growth of trastuzumab-resistant human breast cancer cells via downregulation of akt and beclin-1. *Plos One* 16, e0257298.
- Wu, Y., You, X., Lin, Q., Xiong, W., Guo, Y., Huang, Z., Dai, X., Chen, Z., Mei, S.i., Long, Y., 2022. Exploring the pharmacological mechanisms of xihuang pills against prostate cancer via integrating network pharmacology and experimental validation in vitro and in vivo. *Frontiers in Pharmacology* 12, 791269.
- Yang, J.-L., Lien, J.-C., Chen, Y.-Y., Hsu, S.-C., Chang, S.-J., Huang, A.-C., Amagaya, S., Shinji Funayana, W., Wood, G., Kuo, C.-L., 2016. Crude extract of *Euphorbia formosana* induces apoptosis of DU 145 human prostate cancer cells acts through the caspase-dependent and independent signaling pathway. *Environmental Toxicology* 31, 1600–1611.
- Ye, D., Zhu, Y., 2015. Epidemiology of prostate cancer in China: an overview and clinical implication. *Zhonghua Wai Ke Za Zhi [chinese Journal of Surgery]* 53, 249–252.
- Yu, B.o., Liu, T., Yanxin, D.u., Luo, Z., Zheng, W., Chen, T., 2016. X-ray-responsive selenium nanoparticles for enhanced cancer chemo-radiotherapy. *Colloids and Surfaces b: Biointerfaces* 139, 180–189.
- Yu, J., Qi, H., Wang, Z., Zhang, Z.e., Song, E., Song, W., An, R., 2022. RAB3D, upregulated by aryl hydrocarbon receptor (AhR), promotes the progression of prostate cancer by activating the PI3K/AKT signaling pathway. *Cell Biology International* 46, 2246–2256.
- Zhang, Y., Li, X., Huang, Z., Zheng, W., Fan, C., Chen, T., 2013. 'Enhancement of cell permeabilization apoptosis-inducing activity of selenium nanoparticles by ATP surface decoration', *nanomedicine: nanotechnology. Biology and Medicine* 9, 74–84.
- Zhang, T., Qi, M., Qian, W.u., Xiang, P., Tang, D., Li, Q., 2023. Recent research progress on the synthesis and biological effects of selenium nanoparticles. *Frontiers in Nutrition* 10, 1183487.
- Zhao, S., Qianqian, Y.u., Pan, J., Zhou, Y., Cao, C., Ouyang, J.-M., Liu, J., 2017. Redox-responsive mesoporous selenium delivery of doxorubicin targets MCF-7 cells and synergistically enhances its anti-tumor activity. *Acta Biomaterialia* 54, 294–306.
- Zheng, S., Li, X., Zhang, Y., Xie, Q., Wong, Y.-S., Zheng, W., Chen, T., 2012. PEG-nanolized ultrasmall selenium nanoparticles overcome drug resistance in hepatocellular carcinoma HepG2 cells through induction of mitochondria dysfunction. *International Journal of Nanomedicine* 3939–3949.